Coordinated Space-Based Observations of Equatorial Plasma Bubbles Using TIMED/GUVI and DMSP

Joe Comberiate
Larry Paxton
JHU/APL
June 30, 2009

Introduction

- Plasma bubbles are regions of depleted electron density in the equatorial ionosphere
- Variety of ground and space-based observations can see different aspects of them
- Models of bubble growth exist but they are difficult to predict
- Use UV imaging to reconstruct 3D bubble structure and background electron density
- Characterization improves understanding of bubble origin and evolution

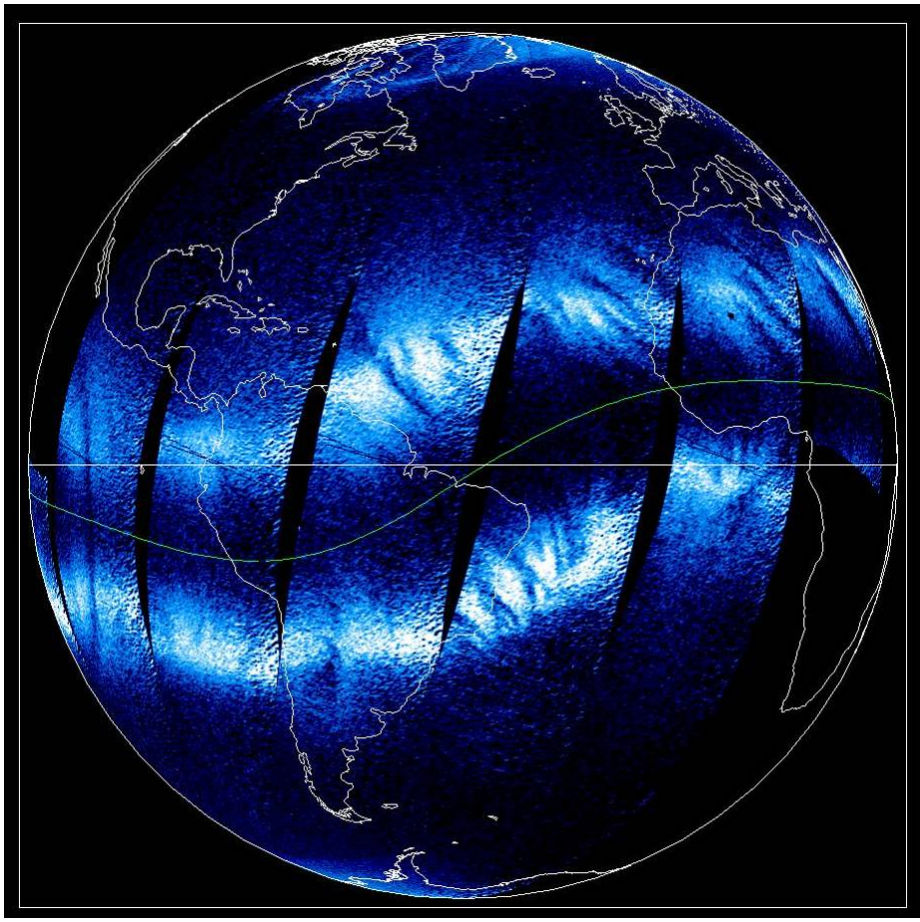

GUVI/SSUSI Disk Imaging

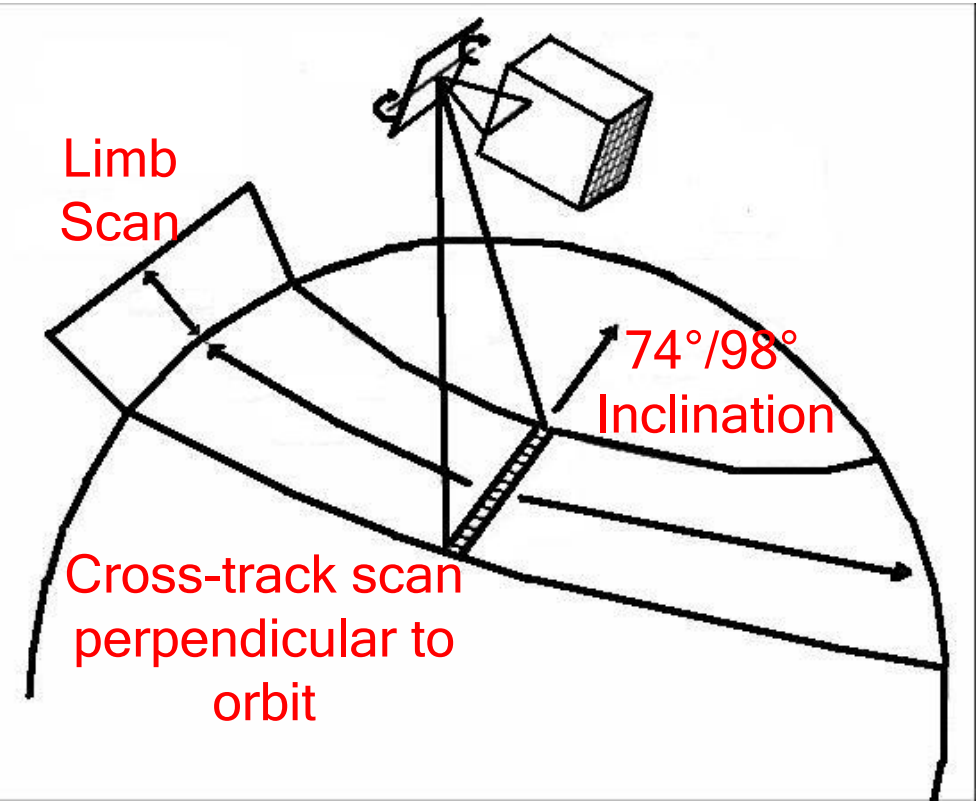

GUVI/SSUSI Disk Imaging

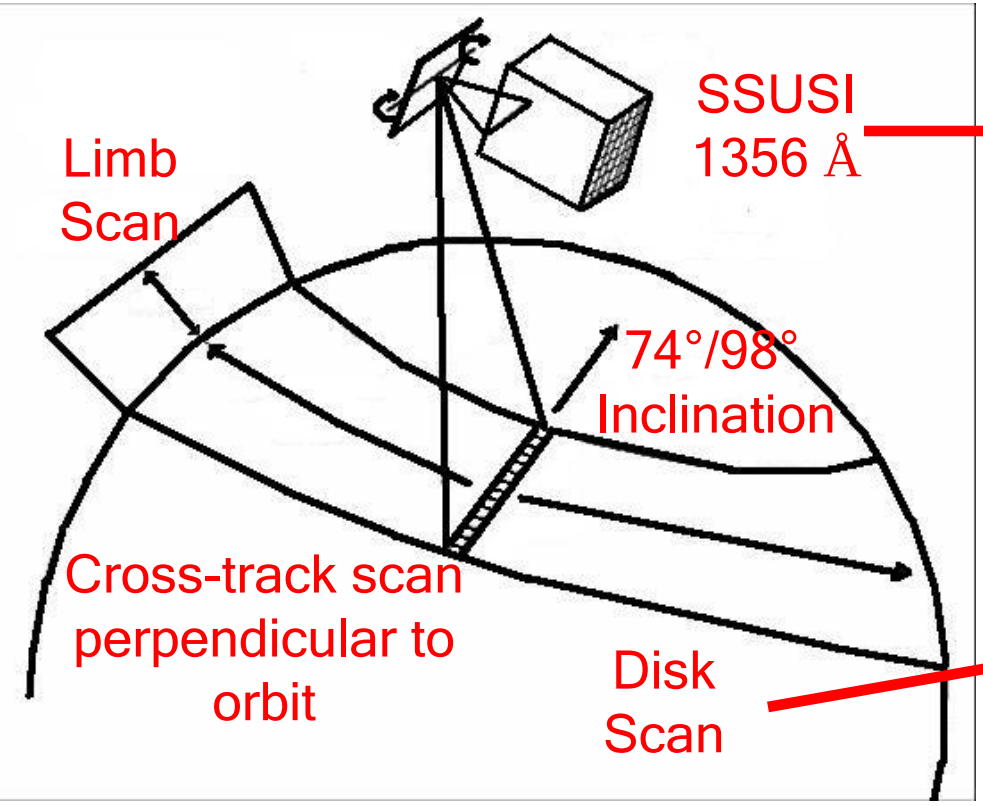

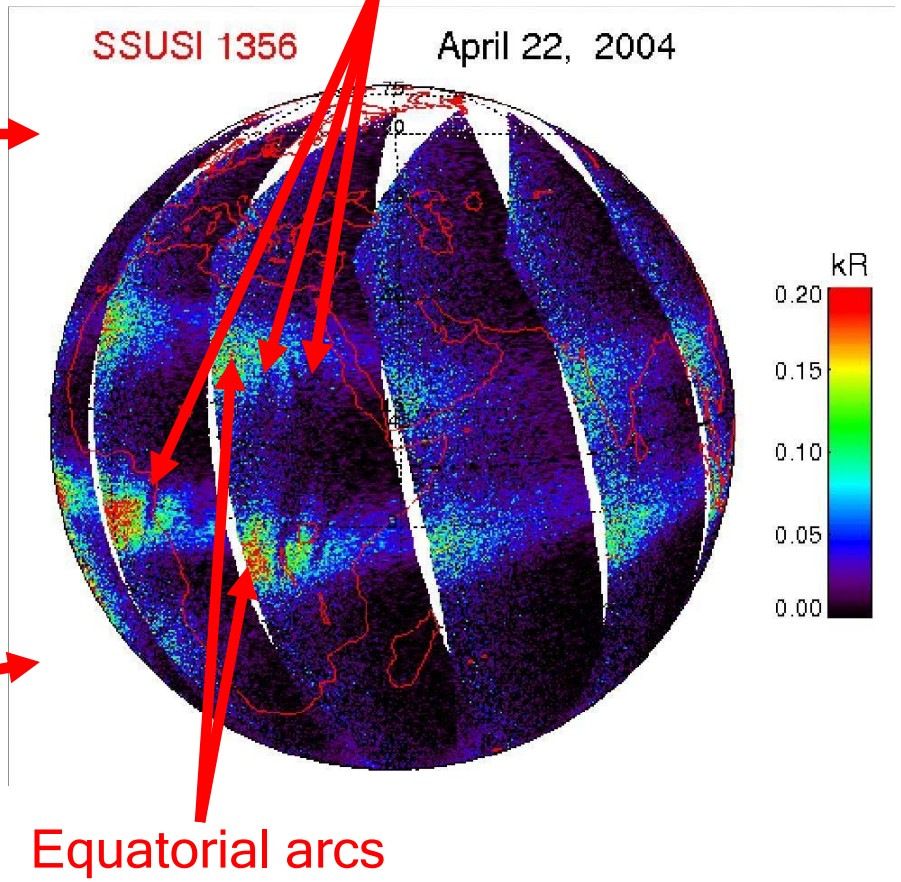

Goal: Recover Altitude Information from LEO Disk Images

- Algorithm for tomographically reconstructing multi-dimensional ionospheric electron density profiles from GUVI or SSUSI disk observations
- Statistical inversion of discrete forward model of UV brightness from ionospheric electron density
- Determine hmF2 and NmF2 of background ionosphere
- Image structure of plasma bubble cross-section perpendicular to magnetic field lines

Primary Tasks for the CEDAR Postdoc Award

2007	Automated Bubble Detection Algorithm GUVI EPB Climatology
2008	SSUSI F16 EPB Imaging SSUSI/GUVI Coordinated Observations

SSUSI Observation Model

- 3-D section of ionosphere along orbit path
- Assume invariance along field lines for that segment
- Distinct overlapping scans with respect to altitude vs. longitude profile allow for tomography

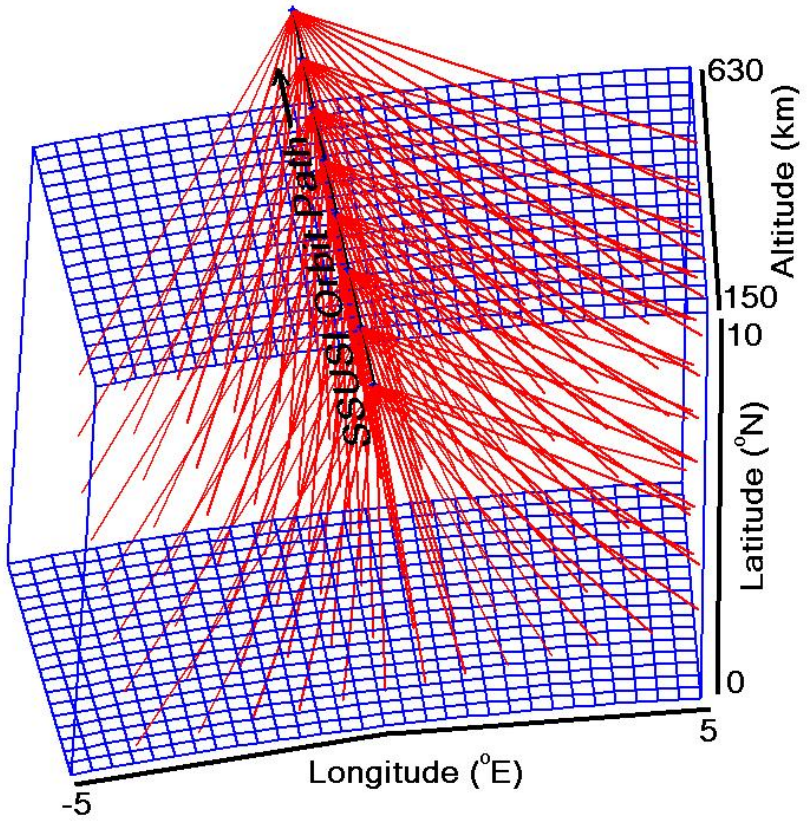

$$I_{1356} \sim \int n_e^2$$

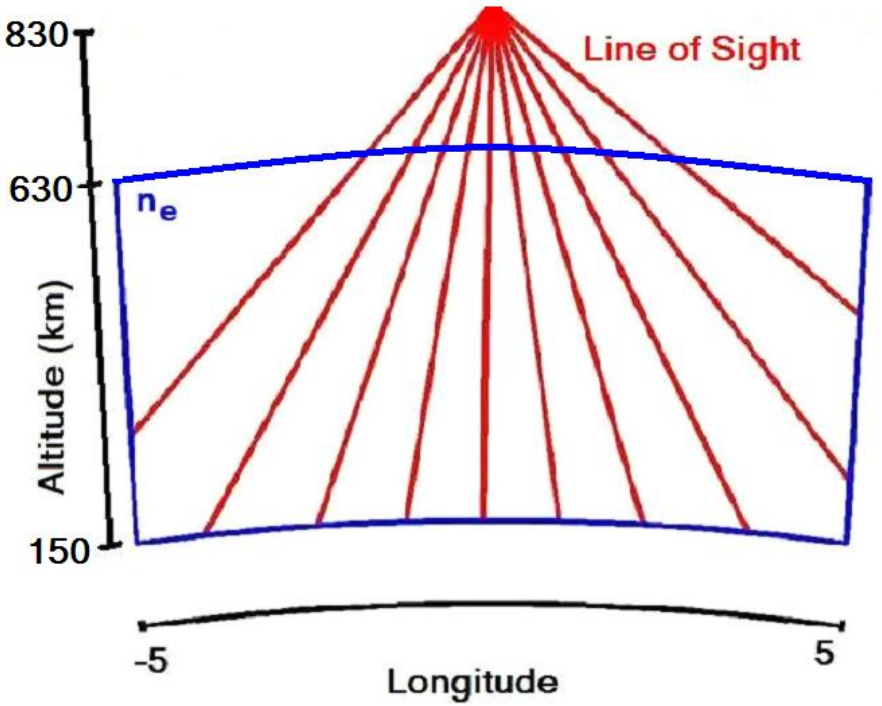

SSUSI Bubble Imaging

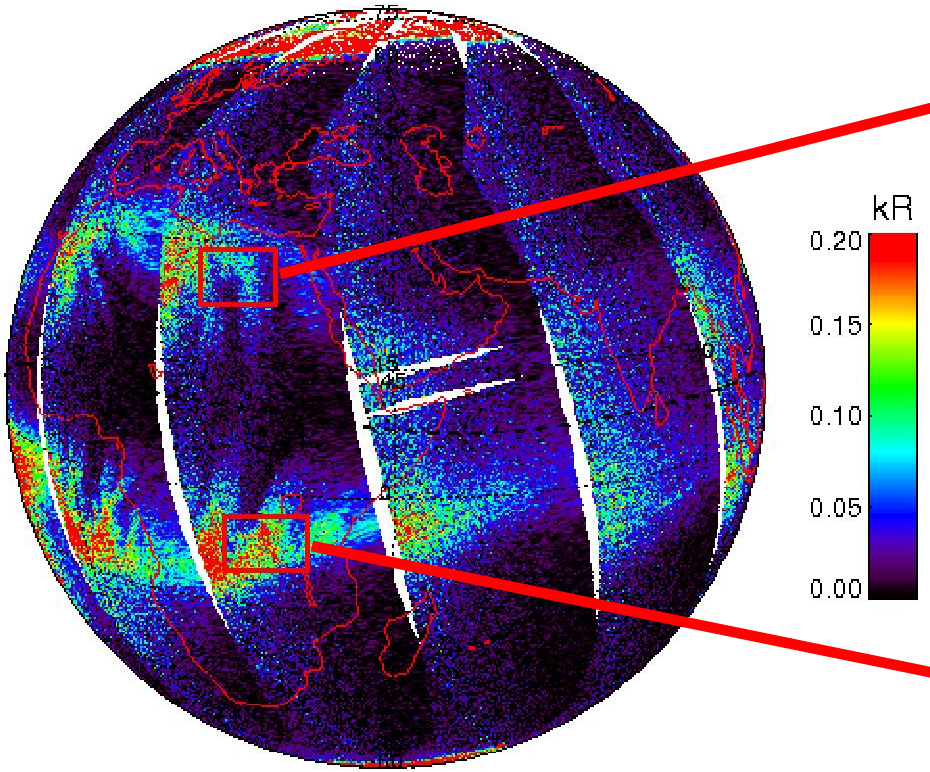

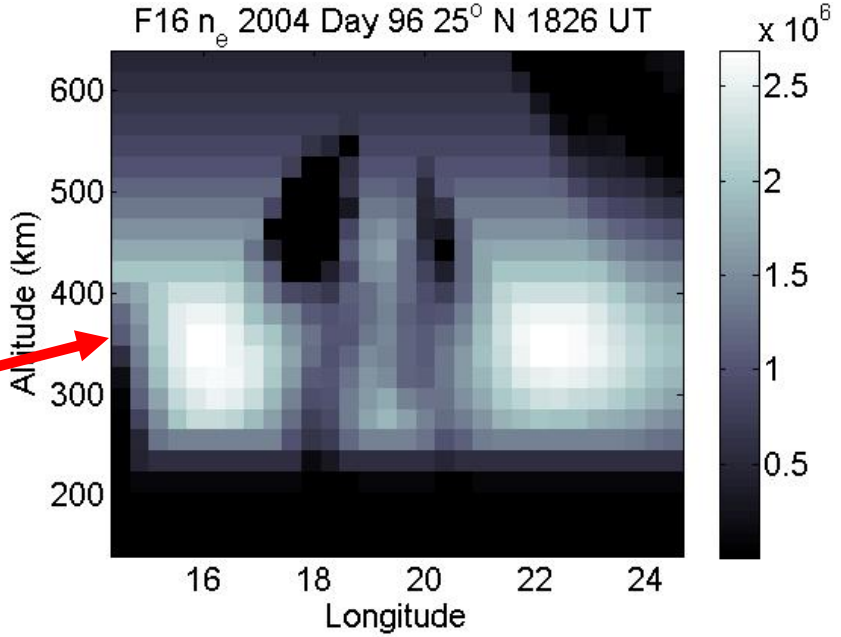

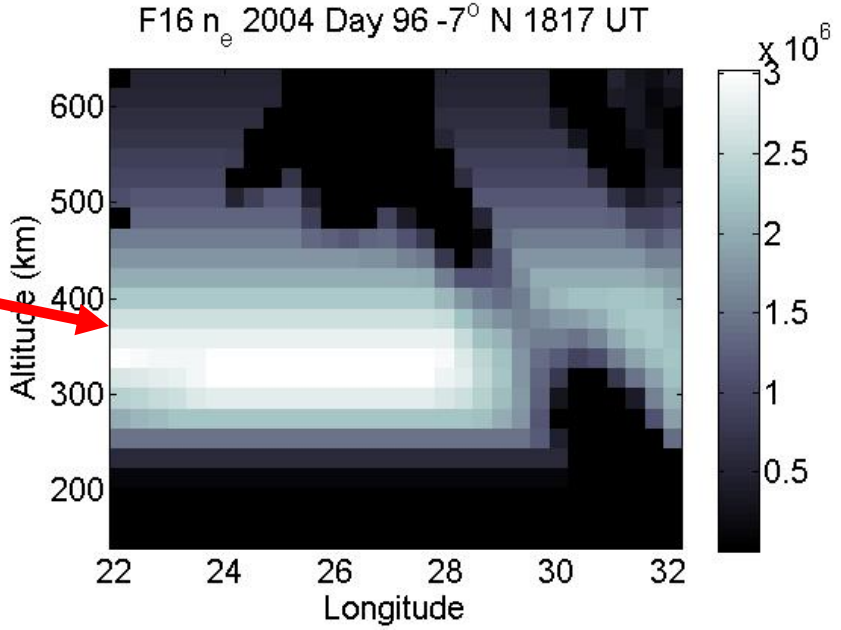

GUVI/SSUSI - Adjoining Images

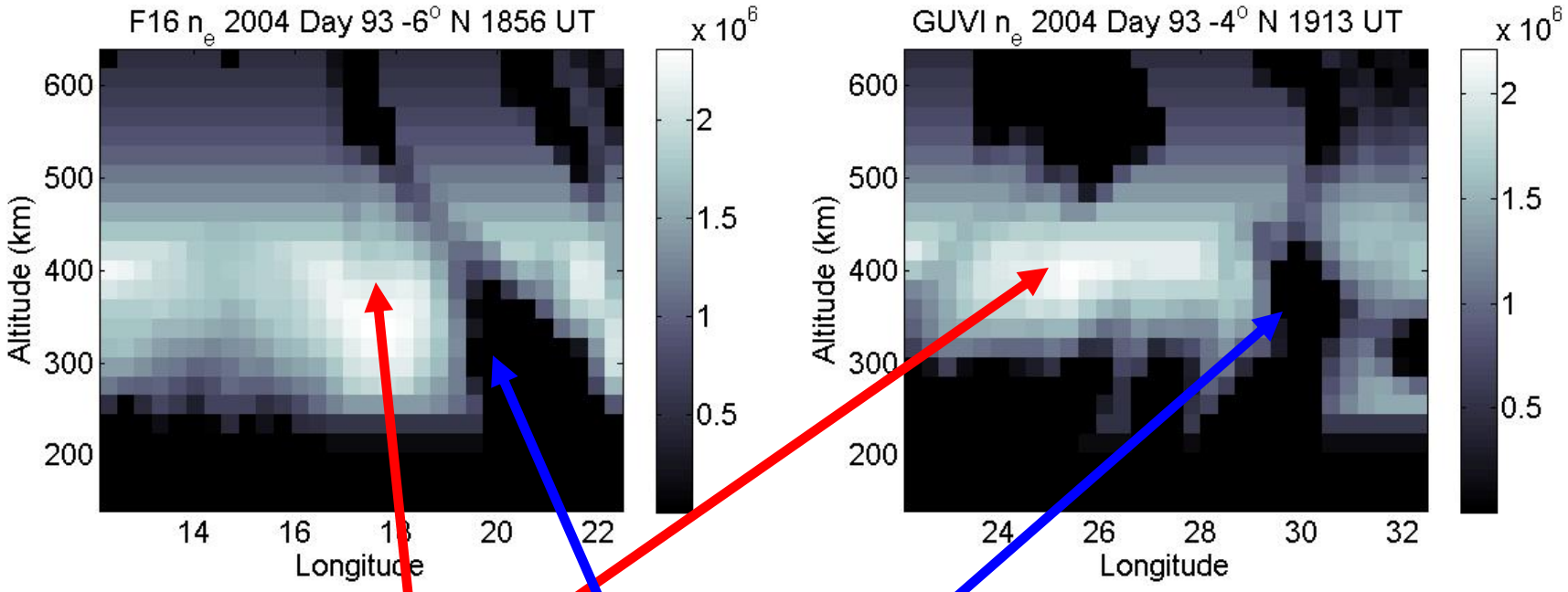

- 20° longitude span covered by two instruments
- hmF2 = 380 km, NmF2 = 2.1×10^6 cm^{-3}
- Multiple plumes visible

Bubble Formation

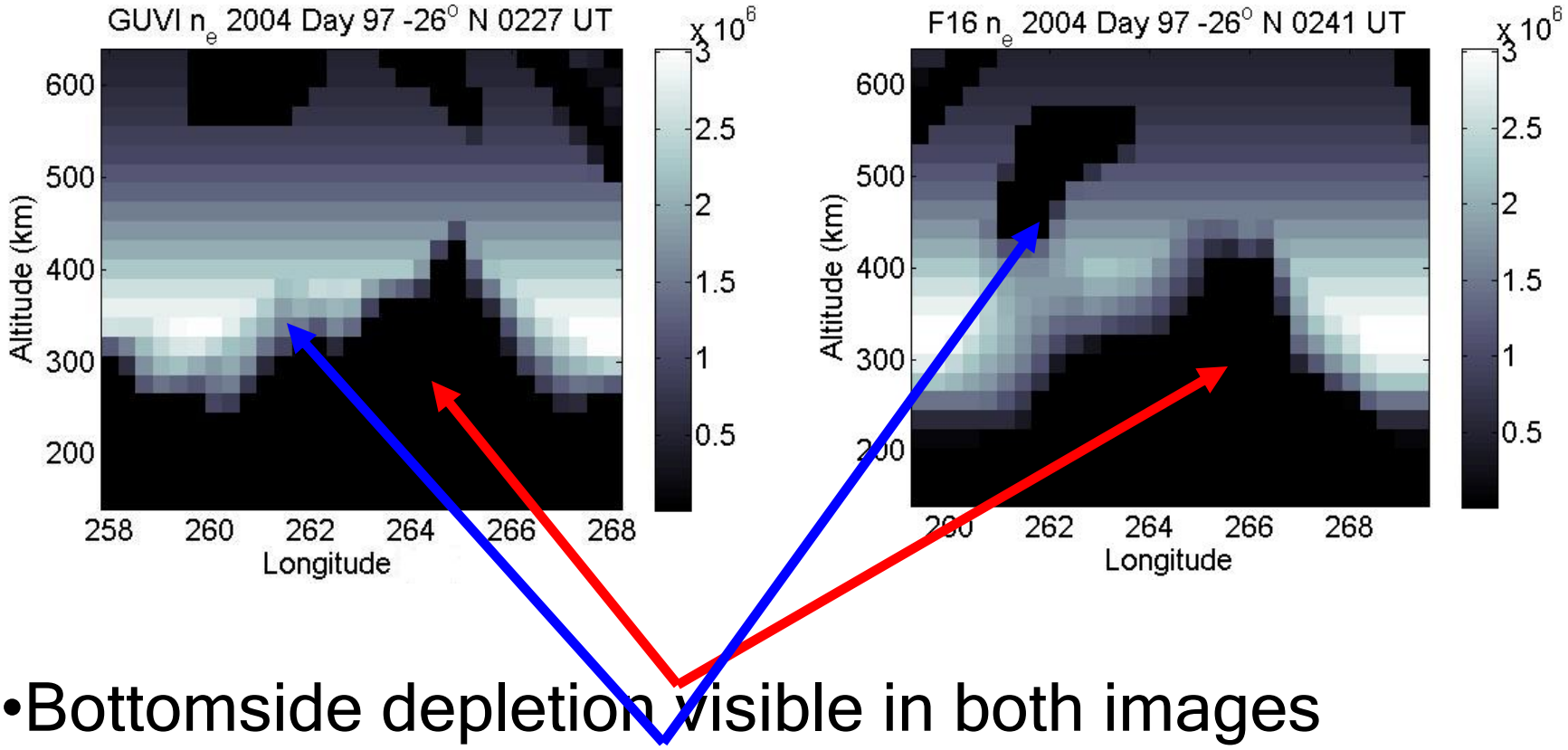

- Bottomside depletion visible in both images
- Plume growth (15 min between images)
- Depleted region drifts East at approx. 100 m/s

Bubble Development

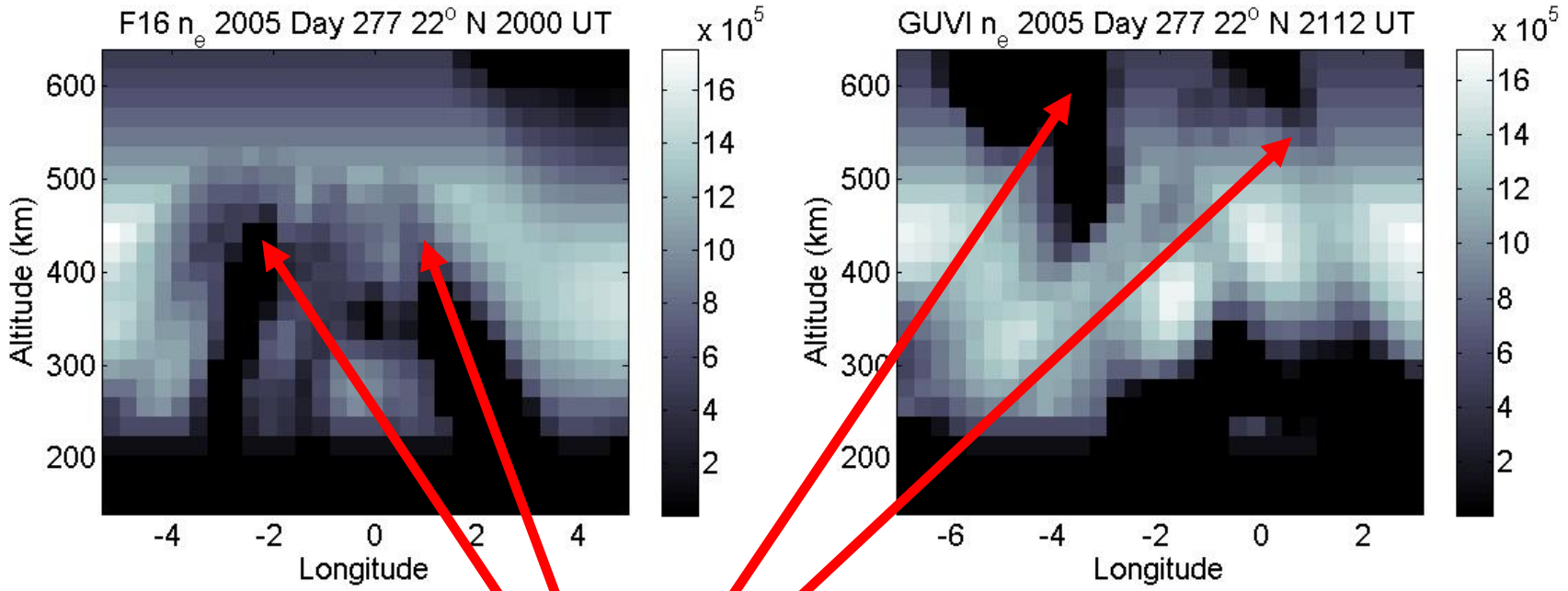

- GUVI image 72 minutes after SSUSI image
- Structures rise from 500 km to above 630 km
- Westward tilt developing in GUVI image
- Thin structures difficult to resolve

3-D Bubble Imaging Technique

- Tomographic inversion performed for each altitude vs. longitude slice
- 12 slices (5° latitude resolution) combined to form 3D profile
- Main sources of error include low SNR for counting statistics, limited latitudinal resolution, and limited-angle viewing geometry

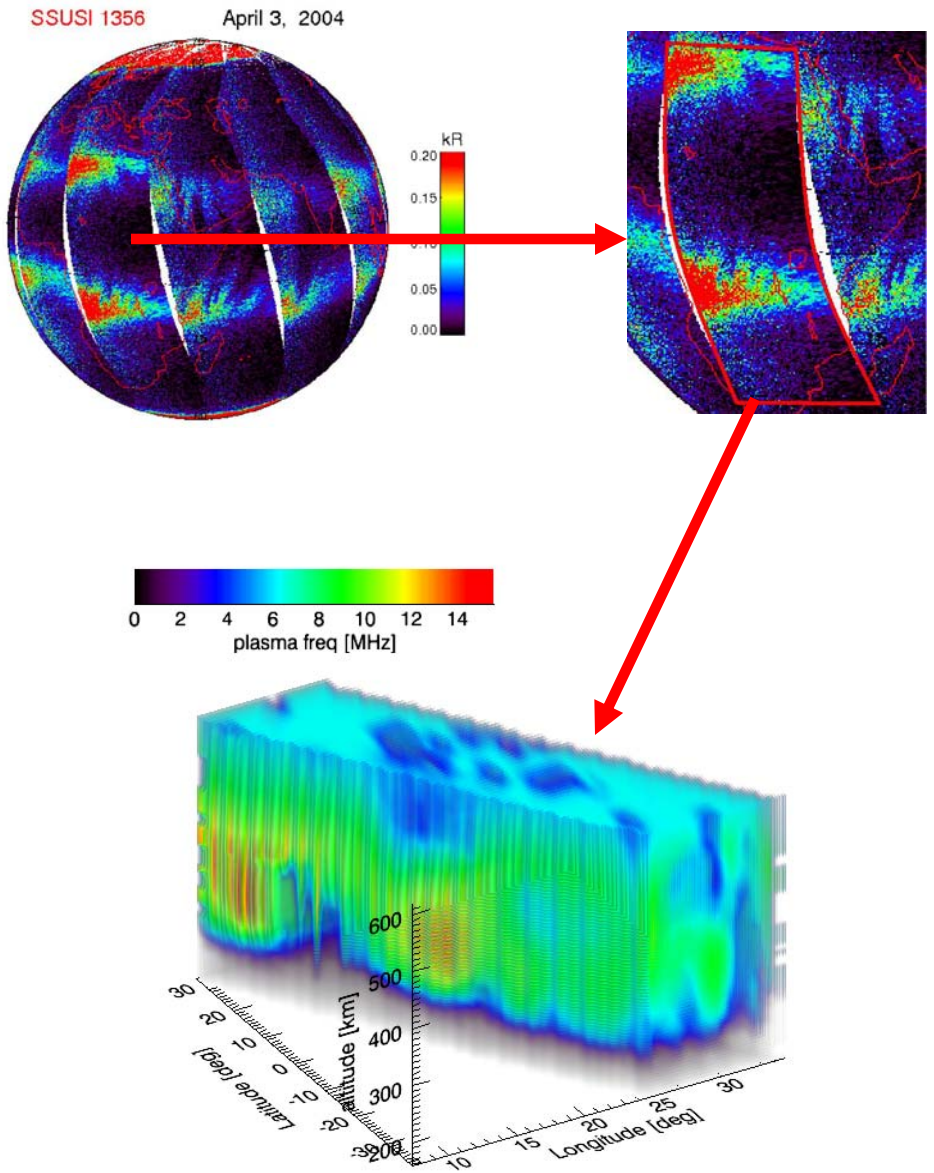

UV Imaging of Sub-Grid Features

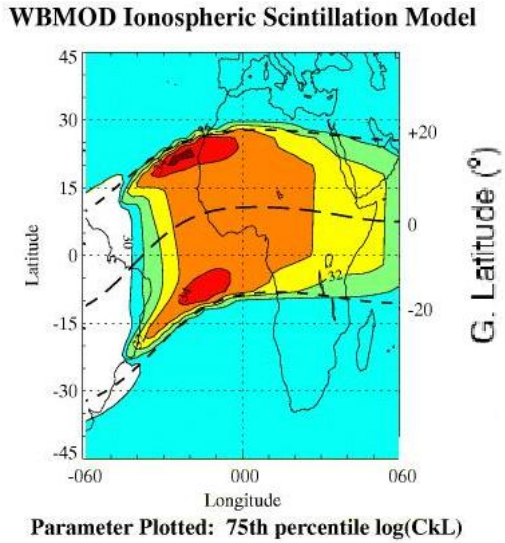

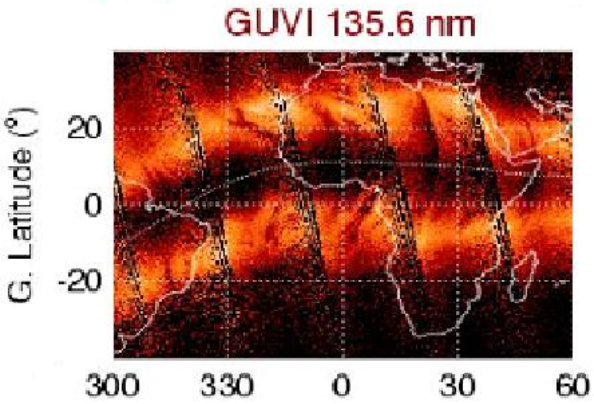

- UV images can locate scintillation-causing depletions
- SSUSI observes sub-grid features not seen by IRI

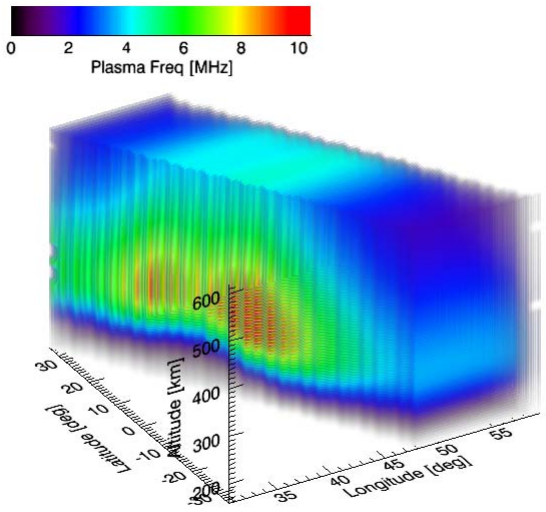

IRI Model Run

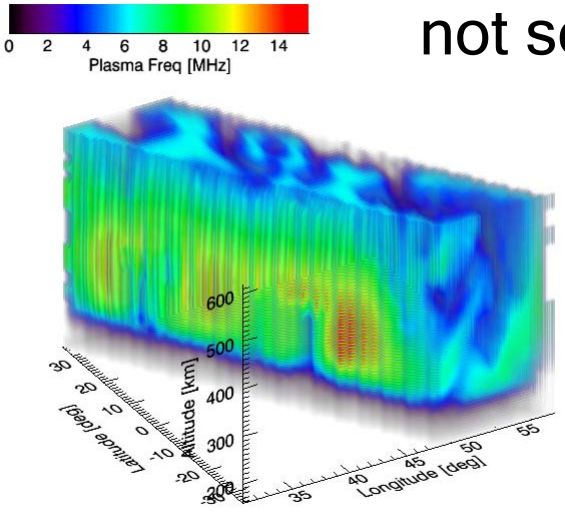

SSUSI 3D Reconstruction

Automated EIA and EPB Detection

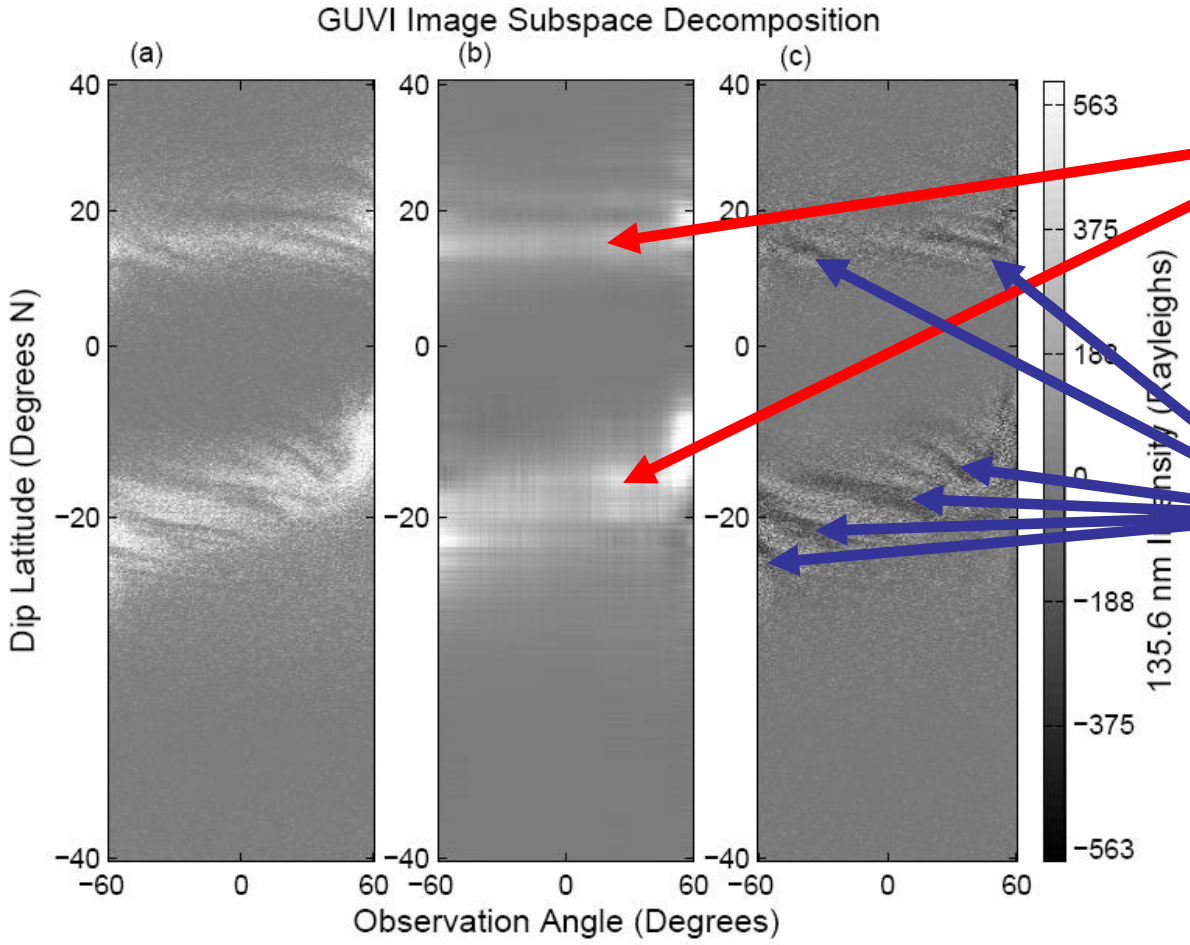

EIA peaks

Plasma bubbles

[from *Henderson* 2006]

- SVD analysis identifies EIA peaks and separates bubbles from background
- Inversions run at North and South EIA peaks

Plasma Bubble Detection

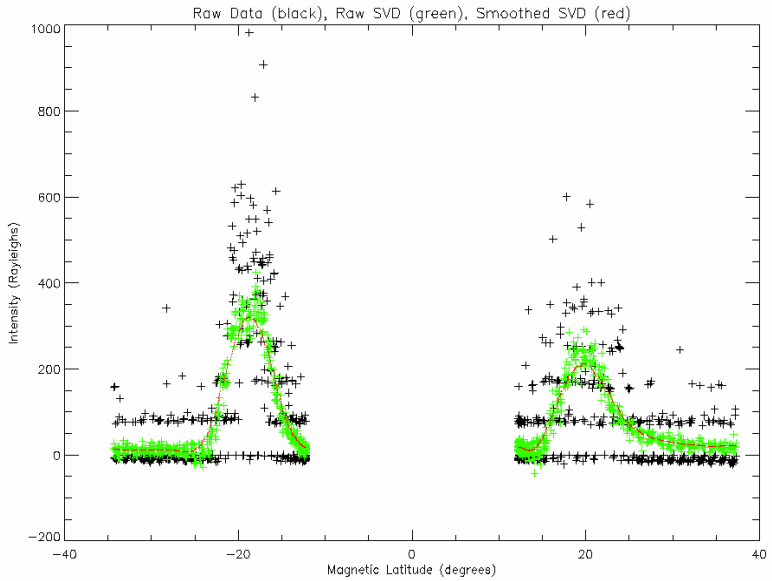

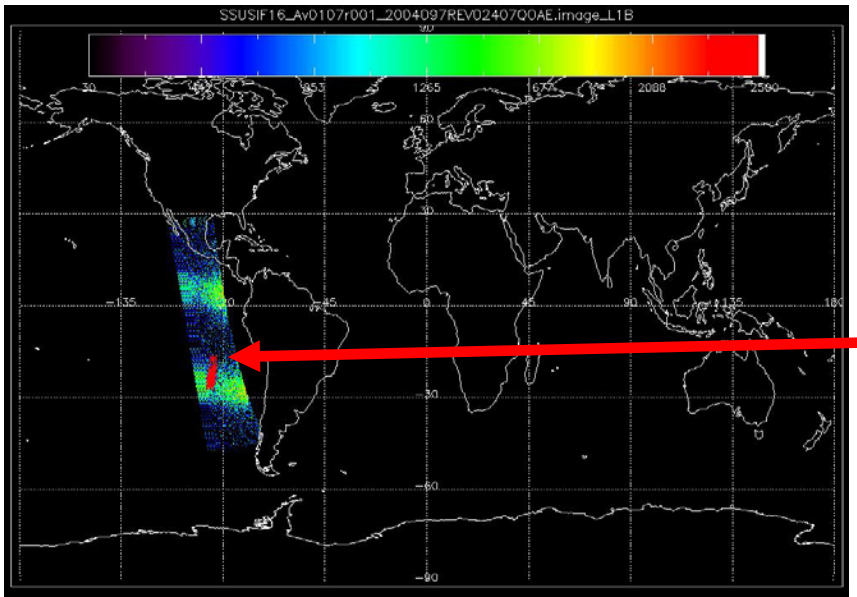

- Automated bubble detection algorithm run on GUVI data from 2002-2007
- Bubble detection algorithm currently being adapted for use with SSUSI data
- Algorithm can locate and characterize EIA peaks
- Pixels containing plasma bubbles are identified

Solar Cycle Effect on EPB Occurrence

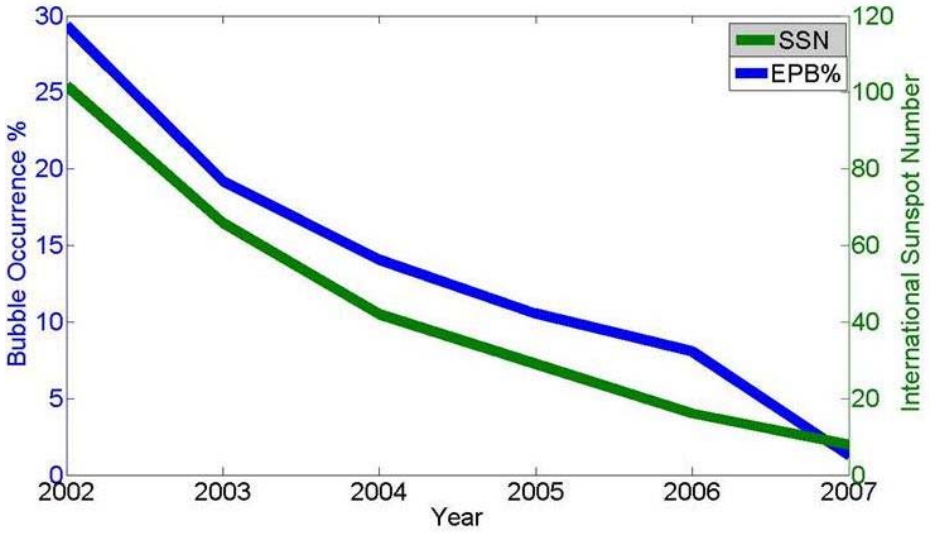

Bubble Occurrence %, 1930-2359 LT

2002 - 29.36%
2003 - 19.19%
2004 - 14.04%
2005 - 10.52%
2006 - 8.05%
2007 - 1.24%

2002 Day 95

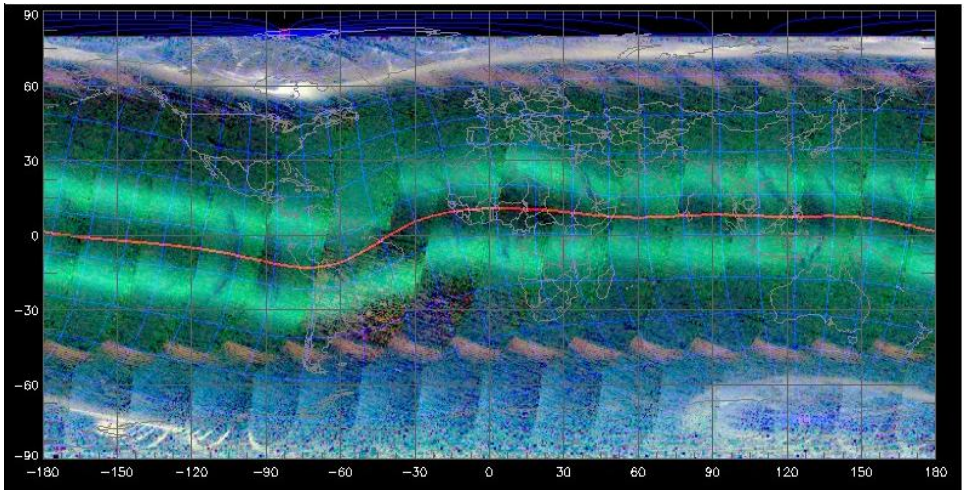

2007 Day 95

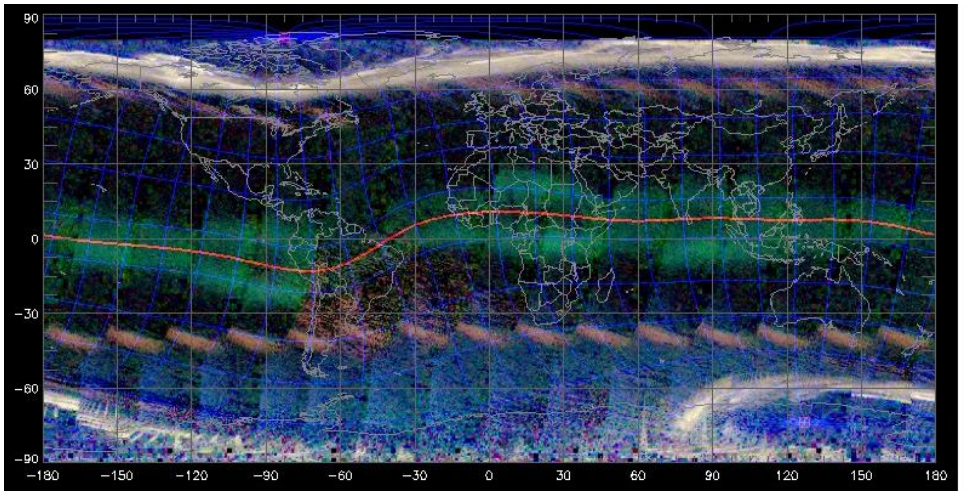

Longitudinal and Seasonal Effects

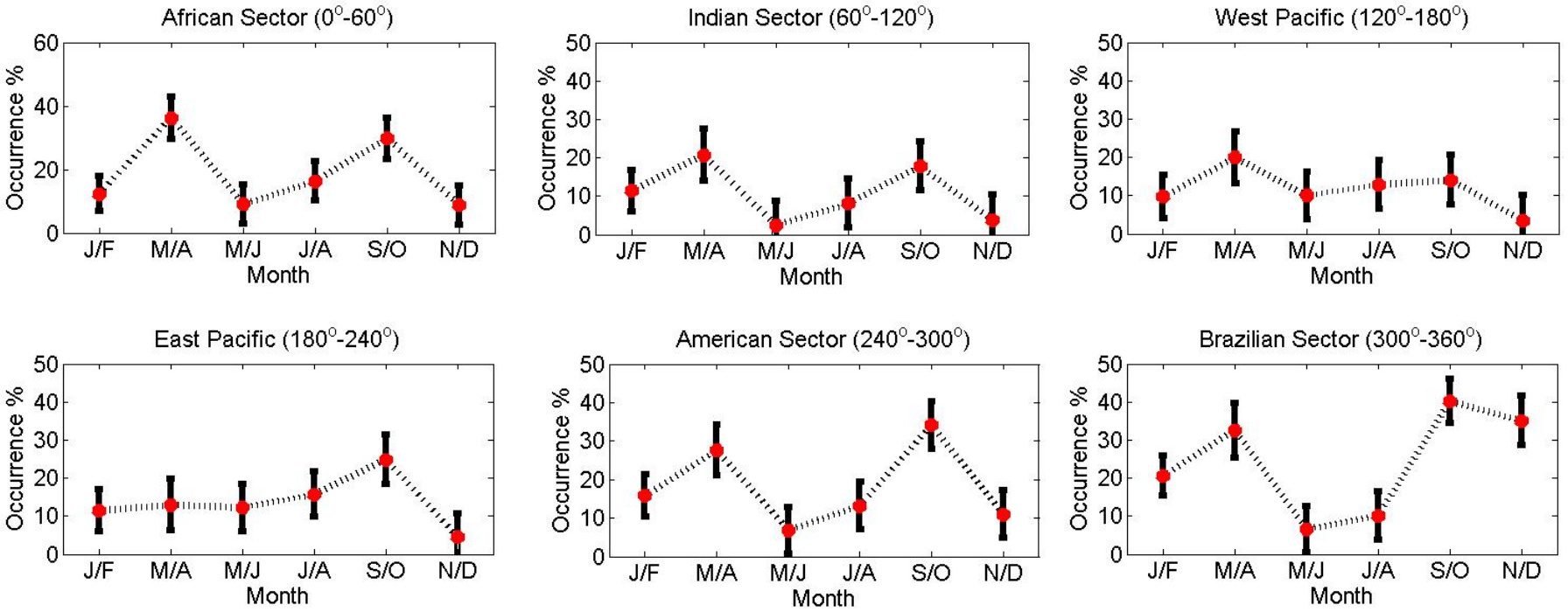

- ESF enhanced in Atlantic Northern winter and Indian equinox
- Maximum activity in Pacific equinox
- Overall ESF activity lowest in Northern summer and greatest in equinoctial periods
- Results consistent with past climatology work

Latitudinal Separation of Arcs

- Latitudinal separation of arcs driven by **ExB** drift
- EPB occurrence maximized at 25°-30° separation

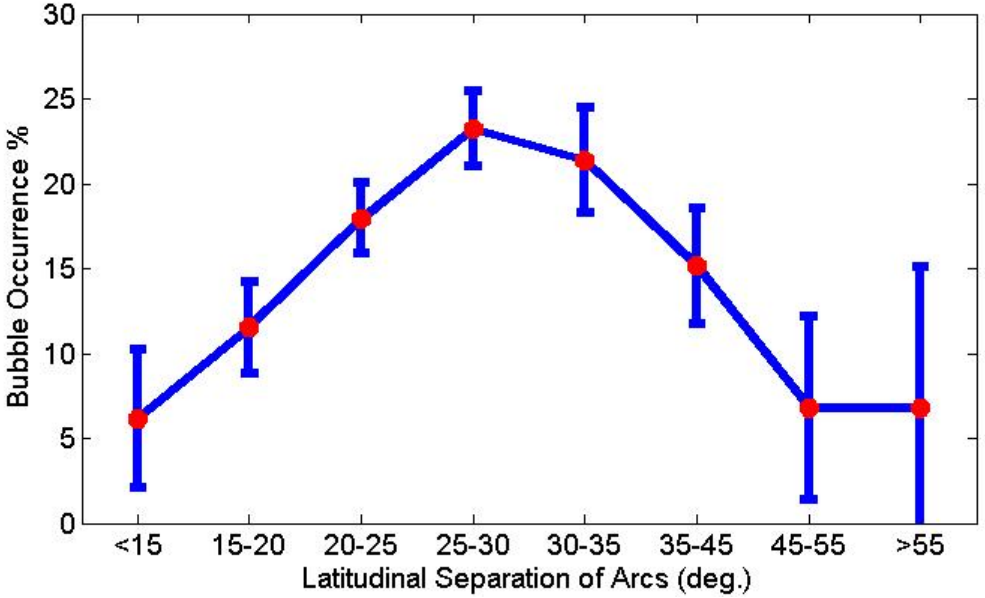

Collapsed arcs, no bubble

Separated arcs with plasma bubble

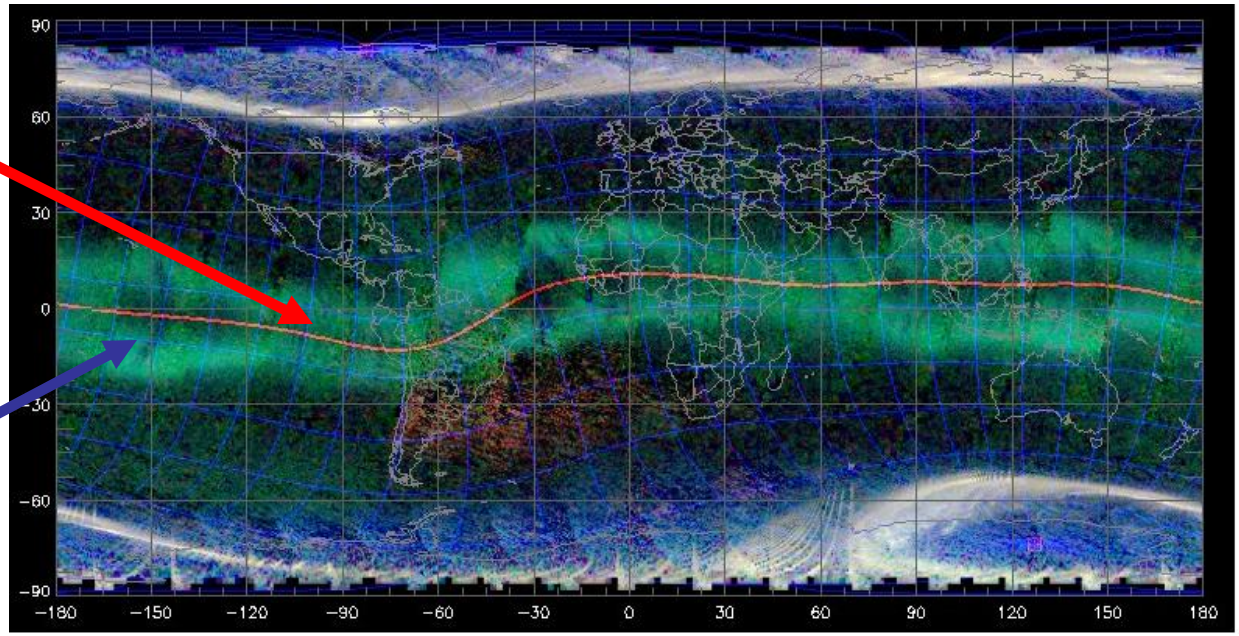

North/South Electron Density Ratio

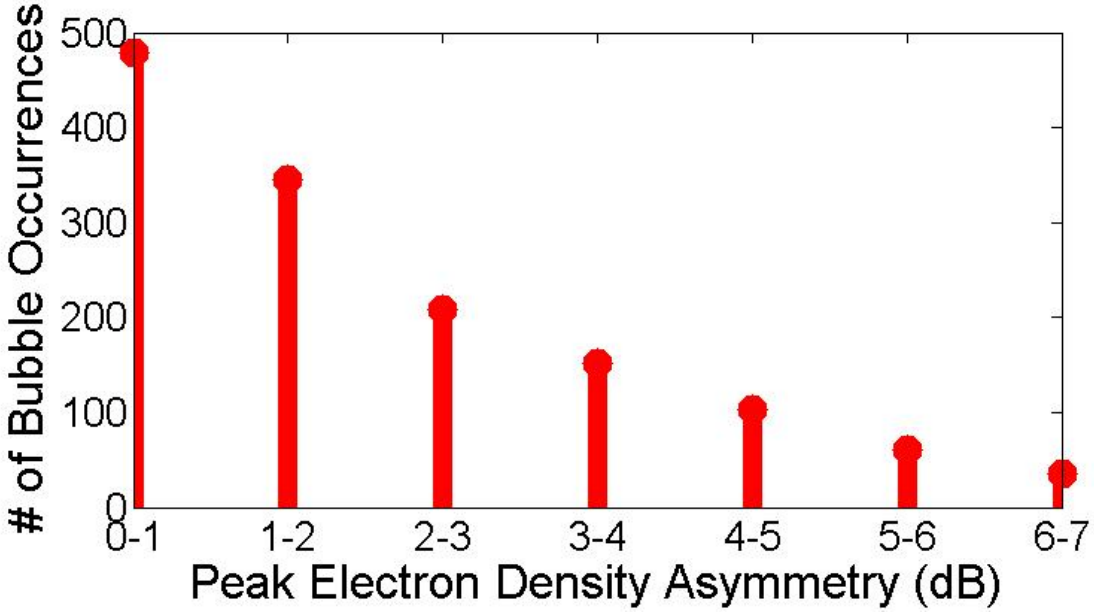

- Electron density profiles reconstructed for northern and southern EIA for each EPB occurrence.
- Peak electron density asymmetry (dB) = $-10\log_{10}\left|\frac{\langle e\rangle_N}{\langle e\rangle_S}\right|$
- More EPB occurrences when EIA peaks are symmetric
- Asymmetry in EIA peaks caused by meridional neutral winds

Discussion

R-T Growth Rate: $\gamma = \frac{\sum_F}{\sum_E + \sum_F}\left[V_p + U_n + \frac{g}{\nu^{eff}}\right]K^F - R$

[from *Sultan 1996*]

E region conductivity

E x B drift term

Vertical electron density gradient

- Alignment of solar terminator with magnetic field lines reduces *E*-region Pedersen conductivity – relates to seasonal/longitudinal variations in growth rate
- Large latitudinal separation of arcs indicates strong **ExB** drift
- Geomagnetic activity and neutral wind effects complicate EPB formation
- UV observations of EIA provide proxy information on conductivities, **ExB** drift, and neutral winds in addition to electron densities.

Conclusions

- Automated bubble detection algorithm locates plasma bubbles for years of GUVI and SSUSI data
- GUVI EPB climatology identifies factors in bubble occurrence – linked to R-T Growth Rate
- SSUSI F16 tomographic model successfully adapted from GUVI, moving towards 3D electron density profiles
- GUVI/SSUSI observe consistent ionosphere in coincident images – observe bubble growth and drift

Many thanks to NSF and CEDAR for supporting this Postdoc!